

Green's Function of a 2-interface photonic system

Daniel Sarcanean*

Universidad Carlos III de Madrid

(Dated: December 13, 2024)

I. INTRODUCTION

During our lectures, we learned that Green's functions are a key mathematical tool in nanophotonics. By describing how a point source generates electromagnetic fields in subwavelength structures, they avoid the need for more complex analytical calculations. In this sense, Green's functions can be thought of as representing the effect of an effective dipole moment, μ .

A. Objectives

Regarding this, it is time for us to get to know how to employ this tool for a very general problem, which is recurrent along the academia. Hence, we have been asked to calculate the Green's function for a two-interface photonic system composed of a metallic slab of thickness t on a dielectric substrate. Specifically, we want to derive an analogous expression for the electric field \mathbf{E} and its local density of states using the general form of $G(r, r', \omega)$ for a dipole source.

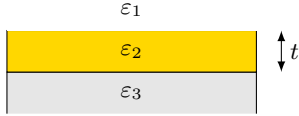


FIG. 1. Simple design of our objective structure.

II. METHODS

In order to develop such calculus, we have employed Python's coding framework, along the libraries `numpy` (general mathematical tool based in C), `matplotlib`, `scipy` (quad and jv, which bring general integration and Bessel functions) and `sqrt` (for complex roots). More information at [this github repository](#).

The simulation criterion has followed the requested proposals. We used a dielectric function of $-10 + 1.2i$ for the metal and 1.45^2 for the dielectric, preserving the nature of the model, all under the assumption of a global wavelength of 550 nm. We specifically designed functions for k_z , $r(\text{pol})$, and G_{ij} to take each component of the Green function matrix and evaluate it separately. As

seen in class, we only had the final form of $G(r, r', \omega)$ to play with:

$$G(r, r', \omega) = \int_0^\infty dk_{\parallel} \frac{k_{\parallel}}{\sqrt{k^2 - k_{\parallel}^2}} e^{i\sqrt{k^2 - k_{\parallel}^2}(z+z')} \times \left\{ \begin{aligned} &r_s(k_{\parallel}, \omega) \begin{bmatrix} \frac{ik_{\parallel}^2}{2} [J_0 + \cos(2\phi)J_2] & \frac{ik_{\parallel}^2}{2} \sin(2\phi)J_2 & 0 \\ \frac{ik_{\parallel}^2}{2} \sin(2\phi)J_2 & \frac{ik_{\parallel}^2}{2} [J_0 + \cos(2\phi)J_2] & 0 \\ 0 & 0 & 0 \end{bmatrix} + \\ &r_p(k_{\parallel}, \omega) \begin{bmatrix} -\frac{ik_{\parallel}^2}{2} [J_0 - \cos(2\phi)J_2] & \frac{ik_{\parallel}^2}{2} \sin(2\phi)J_2 & k_{\parallel}k_z \cos(\phi)J_1 \\ \frac{ik_{\parallel}^2}{2} \sin(2\phi)J_2 & -\frac{ik_{\parallel}^2}{2} [J_0 + \cos(2\phi)J_2] & k_{\parallel}k_z \cos(\phi)J_1 \\ -k_{\parallel}k_z \cos(\phi)J_1 & -k_{\parallel}k_z \cos(\phi)J_1 & ik_{\parallel}^2 J_0 \end{bmatrix} \end{aligned} \right\} \quad (1)$$

III. RESULTS & CONCLUSIONS

The first simulation we performed was an integration of $G(r, r', \omega)$ through z , knowing z reflects the propagation of the field. Choosing values of $r = 30$ nm, $\phi = 0$, $t = 100$ nm and $z' = 50$ nm, we found out the results seen at fig. 2.

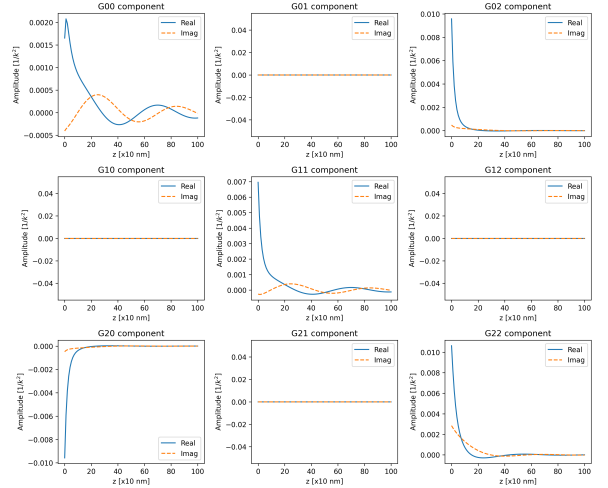


FIG. 2. Expansion of $G(r, r', \omega)$ terms through z .

It is somehow clear that, as r has a certain value, but ϕ is null, the y component of the dipole loses strength ($x = R \cos(\phi)$), so the first component of the Green function, the xx term, ensures that the field propagated along this axis is bigger. This can be correlated with the stronger imaginary part on the first component as well. The peak corresponds precisely to the dipole's location.

Next up, we used another integration to track out the effect of r with a fixed angle $\phi = 0$. This can be seen

* dsarcane@pa.uc3m.es

at fig. 3. Complementary to this, we aroused the same question but for a varying ϕ , which is seen at fig. 4. In the second graph, we standardized along an $r = 30$ nm.

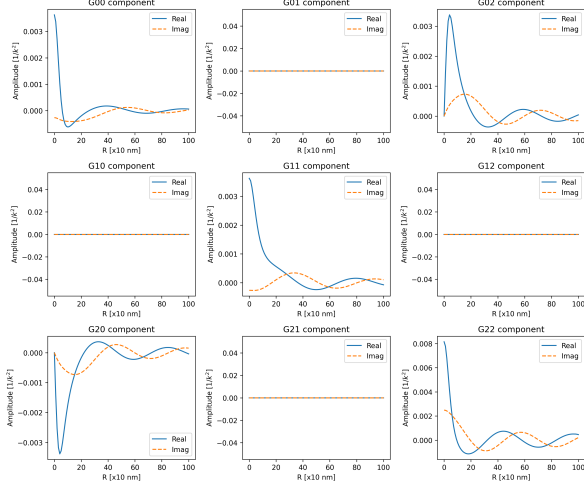


FIG. 3. Expansion of $G(r, r', \omega)$ terms through r .

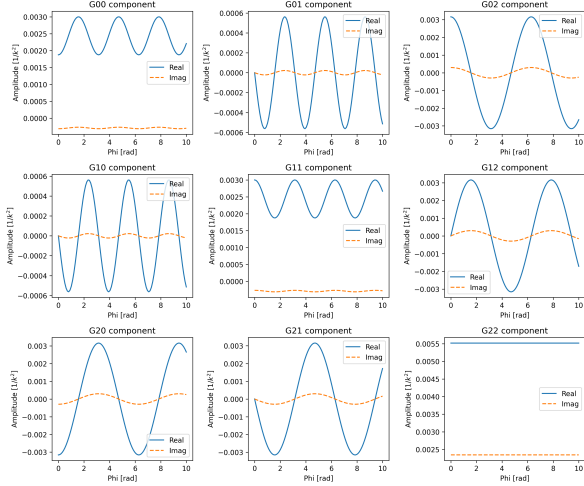


FIG. 4. Expansion of $G(r, r', \omega)$ terms through ϕ .

Some conclusions can be drawn back from these two graphs. First off, we see that the non-diagonal terms along r are conjugate terms. If we put another angle, such as $\phi = \pi/2$, as suggested by the second graph, we would get a fully different drawing off the first plot. Indeed, spatially symmetric terms appear at xy and yx , as seen in fig. 5. This is a proof that the action of the field is correlated through both dimensions for most values of ϕ . In fact, we can see the appearance of some strong resonances at xy and yx au-pair with some peaks at the

other distributions.

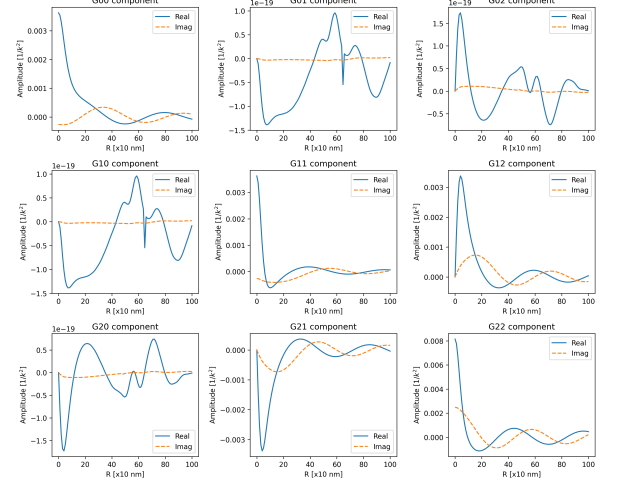


FIG. 5. Expansion of $G(r, r', \omega)$ terms through r with $\phi = \pi/2$.

Another study we commended was to see the effect of a varying thickness, which can be seen at fig. 6. In it, we observe that there are in fact some conditions for which the field's response is homogeneous. One can guess that, for values of t bigger than 30 nm, the response is mostly translated into reflection of the metallic plate, while for smaller dimensions of t , the field is transmitted as for any small enough thin film. The imaginary part, though, resembles more intriguing, and it's probably the result of a localized surface plasmon once the dimensions of the film are small enough to let the incident field to resonate.

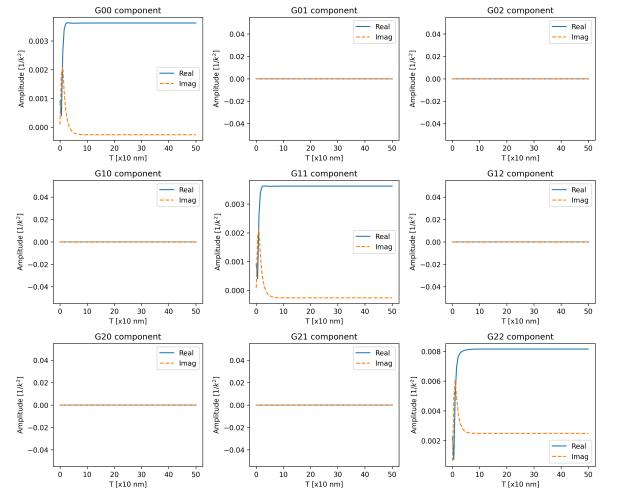


FIG. 6. Expansion of $G(r, r', \omega)$ terms through t .